

Polarization transfer in ${}^4\text{He}(\vec{e}, e' \vec{p})$ and ${}^{16}\text{O}(\vec{e}, e' \vec{p})$ in a relativistic Glauber model

P. Lava, J. Ryckebusch, and B. Van Overmeire

Department of Subatomic and Radiation Physics, Ghent University, Proeftuinstraat 86, B-9000 Gent, Belgium

S. Strauch

Department of Physics, The George Washington University, Washington, D.C. 20052

(Received 30 July 2004; published 20 January 2005)

Polarization-transfer components for ${}^4\text{He}(\vec{e}, e' \vec{p}){}^3\text{H}$ and ${}^{16}\text{O}(\vec{e}, e' \vec{p}){}^{15}\text{N}$ are computed within the relativistic multiple-scattering Glauber approximation (RMSGGA). The RMSGGA framework adopts relativistic single-particle wave functions and electron-nucleon couplings. The predictions closely match those of a relativistic plane-wave model indicating the smallness of the final-state interactions for polarization-transfer components. Also short-range correlations play a modest role for the studied observables, as long as small proton missing momenta are probed in quasielastic kinematics. The predictions with free and various parametrizations for the medium-modified electromagnetic form factors are compared to the world data.

DOI: 10.1103/PhysRevC.71.014605

PACS number(s): 25.30.Dh, 13.40.Gp, 24.10.Jv, 24.70.+s

I. INTRODUCTION

In conventional nuclear physics, nuclei are described in terms of pointlike protons and neutrons, interacting through the exchange of mesons. It has been a long-standing and unresolved issue whether the electromagnetic properties of bound nucleons differ from those of free nucleons. Any sizable modification would have a severe impact on the interpretation of, e.g., the EMC effect [1]. Inclusive $A(e, e')$ data, including their separated longitudinal and transverse cross sections, are rather inconclusive with respect to the allowed ranges for medium modifications. Indeed, a recent reanalysis of the longitudinal inclusive ${}^4\text{He}(e, e')$ response, implementing two-body effects in the nuclear charge operator and realistic wave functions, finds the data consistent with the state-of-the-art calculations when using free-nucleon electromagnetic form factors [2]. To the contrary, an alternate recent reevaluation of the Coulomb sum rule (CSR) concentrating on heavier nuclei discerns it considerably quenched for $A \geq 40$, thereby not excluding sizable medium modifications for the electric form factor $G_E(Q^2)$ [3]. Conversely, a y -scaling analysis of the inclusive $A(e, e')$ data [4] indicates that the medium effects on the magnetic form factor $G_M(Q^2)$ are smaller than 3% for $Q^2 \geq 1$ (GeV/c) 2 . At lower values of the four-momentum transfer Q^2 , a considerably improved description of the separated longitudinal and transverse $A(e, e')$ responses for ${}^{12}\text{C}$ and ${}^{40}\text{Ca}$ was reached after including in-medium $G_E(Q^2)$ and $G_M(Q^2)$ form factors as computed in the Nambu-Jona-Lasinio model [5]. This model is thought to provide a reasonable description of the dynamical breaking of chiral symmetry at nuclear physics scales.

Exclusive $A(e, e' p)$ processes have been put forward as more discriminative than inclusive $A(e, e')$ when it comes to investigating specific aspects of nuclei, and in particular, the possible modifications of the electromagnetic properties attributed to the presence of a medium. Finding signatures of those medium modifications, however, requires an excellent control over all those ingredients of the $A(e, e' p)$ reaction process that are directly related to

the presence of a nuclear medium. They include medium-related effects, such as final-state interactions (FSI), meson-exchange currents (MEC), and isobar currents (IC). We wish to stress that in principle there is a clear distinction among FSI, MEC, and IC effects and those dubbed “medium modifications.” Indeed, the latter refer to medium-driven changes in the internal quark-gluon structure of nucleons. Unfortunately, at the level of the $A(\vec{e}, e' \vec{p})$ observables, no formal distinction can be made among FSI, MEC, and IC effects on one hand and possible medium modifications on the other.

In the 1980s, it was suggested that the ratio of the transverse (T) to the longitudinal (L) response in exclusive $A(e, e' p)$ may provide a handle on the medium modifications of the nucleon’s electromagnetic properties [6,7]. The longitudinal-transverse $A(e, e' p)$ separations suggested substantial deviations from the naive [i.e., plane-wave impulse approximation (PWIA)] predictions for the T/L ratio. The data for medium-heavy nuclei such as ${}^{12}\text{C}$ and ${}^{40}\text{Ca}$, however, could be satisfactorily explained after implementing FSI mechanisms [8], thereby adopting free-nucleon electromagnetic form factors. For the ${}^4\text{He}$ nucleus, charge-exchange processes turned out to be of great importance to explain the measured T/L ratios [9–11]. The above-mentioned findings indicate that medium modifications of the electromagnetic form factors are apparently modest and support the picture that despite their substructure, nucleons are rather robust objects.

For a long time, Rosenbluth separations in elastic electron-proton scattering were the sole source of information about free-proton electromagnetic form factors. Continuing efforts to improve on the quality of electron beams and hadron detection, however, made precise measurements of polarization degrees-of-freedom a viable option to address issues in hadronic physics with the aid of the electromagnetic probe. In polarized electron free-proton scattering $\vec{e}(E_e) + p \rightarrow e'(E_{e'}) + \vec{p}$, the ratio of the electric [$G_E(Q^2 = -q^\mu q_\mu)$] to the magnetic [$G_M(Q^2)$] Sachs form factors, can be extracted from the

following [12]:

$$\frac{G_E(Q^2)}{G_M(Q^2)} = -\frac{P'_x}{P'_z} \frac{E_e + E_{e'}}{2M_p} \tan\left(\frac{\theta_e}{2}\right). \quad (1)$$

Here, q^μ is the four-momentum transfer, P'_x and P'_z are the transferred polarization in the direction perpendicular to and parallel with the three-momentum transfer, and θ_e is the electron scattering angle.

Of all observables accessible in $A(e, e'p)$, the transferred polarization components P'_i have been recognized as the ones with the weakest sensitivity to FSI, MEC, and IC distortions [13–18]. Therefore, polarization-transfer components have been put forward as a tool to examine the magnitude of the in-medium electromagnetic form factors. Hereby, one adopts the philosophy that the in-medium (or off-shell) electron-proton vertex Γ^μ has the same Lorentz structure as the free-proton one. This is the so-called impulse approximation (IA), which has been successfully applied in a vast number of calculations. Investigations search for anomalous behavior, which manifests itself as a deviation between up-to-date calculations and well-controlled observables obtained in optimized kinematic conditions. Possible anomalous behavior of this kind may subsequently be interpreted as an indication for a medium effect. The described procedure is a pragmatic one and may be subject to criticism, particularly in view of the ambiguities with respect to describing the off-shell Γ^μ vertex [19].

Recently, $(\vec{e}, e'\vec{p})$ measurements for the target nuclei ^{16}O [20] and ^4He [21,22] have been reported. The $^{16}\text{O}(\vec{e}, e'\vec{p})$ measurements have been confronted to various nonrelativistic and relativistic calculations [23–27]. All these calculations utilize an optical potential to incorporate the FSI. The calculations of Ref. [26] indicate that two-nucleon currents such as MEC and IC affect the polarization-transfer components in ^{16}O to less than 5% provided that missing momenta below 200 MeV/c are probed. The nonrelativistic calculations of Ref. [23] attributed somewhat larger corrections to the two-nucleon currents, in particular for proton knockout from the $p3/2$ and $s1/2$ shells. All calculations, however, predict similar trends for the MEC and IC corrections on the polarization-transfer components. One major finding is that their effect dwindles with increasing Q^2 and decreasing missing momentum. Relativistic effects on the transferred polarizations P'_x and P'_z have been investigated in Refs. [24,27] and are discerned at the few percentage levels as long as the probed missing momentum remains relatively small ($p_m \leq 200$ MeV/c). These studies also indicated that at higher missing momenta the uncertainties stemming from off-shell ambiguities are larger than the overall impact of the relativistic effects. Apparently, all theoretical investigations indicate that when probing low missing momenta in quasielastic kinematics, the effect on the polarization-transfer components of typical medium-related complications such as MEC, IC, and off-shell ambiguities can be kept under reasonable control.

In Ref. [22] the Jefferson Laboratory (JLAB) $^4\text{He}(\vec{e}, e'\vec{p})$ data, which cover the range $0.5 \leq Q^2 \leq 2.6$ (GeV/c)², are compared to the state-of-the-art relativistic distorted-wave impulse approximation (RDWIA) calculations of Udías

et al. [28]. This model provided a better overall description of the data when implementing medium-modified electromagnetic form factors as predicted in the quark-meson coupling (QMC) model [29–31]. At JLAB, exclusive $A(e, e'p)$ studies are conducted in a kinematic regime that may outreach the range of applicability of optical-potential approaches for describing FSI mechanisms. Indeed, given the highly inelastic and diffractive nature of proton-nucleon scattering at proton lab momenta exceeding 1 GeV/c, the use of optical potentials for modeling FSI seems rather unnatural. For example, for the $Q^2 = 2.6$ (GeV/c)² case, the $^4\text{He}(\vec{e}, e'\vec{p})$ data of Ref. [22] are compared to RDWIA calculations with extrapolated optical potentials.

At higher energies, Glauber multiple-scattering theory provides a more natural and economical description of FSI mechanisms [32–34]. A typical Glauber model is based on the eikonal approximation and the assumption of consecutive cumulative scattering of a fast proton on a composite target of $A - 1$ “frozen” nucleon scatterers. Recently, we developed a relativistic version and dubbed it as the relativistic multiple-scattering Glauber approximation (RMSGGA) [35–37]. The RMSGGA heavily draws on ingredients of standard RDWIA $A(e, e'p)$ approaches. For example, the assumptions made with respect to the construction of the bound-state wave functions and electromagnetic couplings are identical in RDWIA and RMSGGA. The sole difference concerns the construction of the scattering wave function. In RDWIA one adopts the philosophy that optical potentials parametrizing the FSI mechanisms in elastic $A(p, p)A$ processes, can also be utilized to model the impact of the proton’s distortions in $A(e, e'p)$ reactions. In a Glauber framework, conversely, the effects of FSI are computed directly from nucleon-nucleon scattering data. Despite the dissimilar assumptions underlying the treatment of FSI, it has been recently shown that the RMSGGA and RDWIA predictions for the nuclear transparencies extracted from $A(e, e'p)$ are alike in an intermediate proton kinetic-energy range where both optical-potential and Glauber approaches are judged to be applicable [38]. The RMSGGA $A(e, e'p)$ model has a number of virtues, including the fact that it is unfactorized, which means that our cross section is not written in terms of the product of an off-shell electron-proton cross section and a distorted missing momentum distribution. In addition, our implementation adopts the full-fledged multiple-scattering version of the Glauber approach and describes each nucleon scattering center in the residual nucleus with its particular single-particle wave function. Thereby, we avoid a frequently adopted averaging approximation that allows introducing the nuclear density.

In this article, RMSGGA predictions for the polarization-transfer components in ^4He and ^{16}O are presented and compared to the world data. The numerical calculations are performed with both free and medium-modified electromagnetic form factors. For the latter we use the predictions of the QMC model [29–31] and of a modified Skyrme model [39,40]. It is the purpose of this article to address the questions whether a Glauber approach can adequately describe the $(\vec{e}, e'\vec{p})$ polarization-transfer components and to what extent its predictions differ from typical distorted-wave (or optical-potential) approaches.

The outline of this article is as follows. In Sec. II A the basic features of the RMSGA formalism are sketched. Section II B presents predictions for the medium-modified electromagnetic form factors from some specific nucleon models and outlines how these form factors are implemented in the calculation of the polarization-transfer components. Section III presents our numerical results. We summarize our findings and state our conclusions in Sec. IV.

II. FORMALISM

In this section, we first review the basic ingredients that enter the RMSGA formalism [37]. Next, the method of implementing medium-modified electromagnetic form factors is outlined.

A. RMSGA model

Adopting the IA and the independent-nucleon picture, the basic quantity to be computed in a relativistic approach to $A(e, e' p)$ is the transition matrix element

$$\langle J^\mu \rangle = \int d\vec{r} \bar{\phi}_F(\vec{r}) \hat{J}^\mu(\vec{r}) e^{i\vec{q}\cdot\vec{r}} \phi_\alpha(\vec{r}), \quad (2)$$

where ϕ_α and ϕ_F are the relativistic bound-state and scattering wave functions. Further, \hat{J}^μ is the relativistic one-body current operator modeling the coupling between the virtual photon and a nucleon embedded in the medium. The relativistic bound-state wave functions are obtained within the Hartree approximation to the σ - ω model [41]. As discussed by Walecka [42], the quantum-field theory can be approximated by replacing the meson field operators with their expectation values. The resulting eigenvalue equations of the relativistic mean-field theory can be solved exactly. The corresponding bound-state wave functions ϕ_α are four-spinors and can be formally written as follows:

$$\phi_\alpha(\vec{r}, \vec{\sigma}) = \begin{pmatrix} \frac{iG_{n\kappa\alpha}(r)}{r} \mathcal{Y}_{\kappa_\alpha m_\alpha}(\Omega_r, \vec{\sigma}) \\ -\frac{F_{n\kappa\alpha}(r)}{r} \mathcal{Y}_{-\kappa_\alpha m_\alpha}(\Omega_r, \vec{\sigma}) \end{pmatrix}, \quad (3)$$

with $\mathcal{Y}_{\kappa_\alpha m_\alpha}(\Omega_r, \vec{\sigma})$ the usual spin spherical harmonics. In a high-resolution and exclusive $A(e, e' p)$ experiment, the angular momentum of the state in which the $A - 1$ residual nucleus is left determines the quantum numbers $\alpha \equiv (n_\alpha, \kappa_\alpha, m_\alpha)$. In determining the bound-state wave functions, all results contained in this work use the W1 parametrization [43] for the different field strengths. Further, we adopt the Coulomb gauge and the current operator in its CC2 form [44]

$$J^\mu(\vec{r}) = F_1^p(Q^2) \gamma^\mu + F_2^p(Q^2) i \frac{\kappa_p}{2m_p} \sigma^{\mu\nu} q_\nu. \quad (4)$$

In computing the matrix elements, the q^μ is evaluated in the laboratory frame and the energy transfer is based on electron-scattering kinematics.

We now turn to the question of how to determine a relativistic scattering wave function for the emitted proton. Traditionally, the Glauber approach relies on a number of assumptions: first, the use of the eikonal approximation and,

further, the so-called frozen approximation. The latter allows one to formulate a full-fledged multiple-scattering theory for the emission of a ‘‘fast’’ proton from a composite system consisting of $A - 1$ frozen nucleons. In Ref. [37], a relativistic and unfactorized formulation of Glauber multiple-scattering theory has been outlined. In this approach, termed RMSGA, the scattering wave function in the matrix element of Eq. (2) takes on the following form:

$$\phi_F(\vec{r}) \equiv \phi_{pF, sF}(\vec{r}) \mathcal{G}(\vec{b}, z), \quad (5)$$

where $\phi_{pF, sF}$ is a relativistic plane wave. The impact of the FSI mechanisms on the scattering wave function is contained in the scalar Dirac-Glauber phase $\mathcal{G}(\vec{b}, z)$

$$\mathcal{G}(\vec{b}, z) = \prod_{\alpha \neq \alpha_1} \left[1 - \int d\vec{r}' |\phi_\alpha(\vec{r}')|^2 \theta(z' - z) \Gamma(\vec{b} - \vec{b}') \right], \quad (6)$$

where the product over $\alpha(n, \kappa, m)$ extends over all occupied single-particle states in the target nucleus, not including the one (here denoted as α_1) from which the proton is ejected. The profile function for pN scattering is defined in the standard manner

$$\Gamma(\vec{b}) = \frac{\sigma_{pN}^{\text{tot}}(1 - i\epsilon_{pN})}{4\pi\beta_{pN}^2} \exp\left(\frac{-b^2}{2\beta_{pN}^2}\right). \quad (7)$$

The parameters σ_{pN}^{tot} , β_{pN} , and ϵ_{pN} depend on the proton energy and fitted values to the pN data can be found in Ref. [45].

The Dirac-Glauber phase $\mathcal{G}(\vec{b}, z)$ of Eq. (6) can be cast in the following form:

$$\begin{aligned} \mathcal{G}(\vec{b}, z) = & \prod_{\alpha(n, \kappa, m) \neq \alpha_1(n_1, \kappa_1, m_1)} \left\{ 1 - \frac{\sigma_{pN}^{\text{tot}}(1 - i\epsilon_{pN})}{4\pi\beta_{pN}^2} \int_0^\infty b' db' \right. \\ & \times \int_{-\infty}^{+\infty} dz' \theta(z' - z) \left[\left(\frac{G_{n\kappa}(r'(b', z'))}{r'(b', z')} \mathcal{Y}_{\kappa m}(\Omega', \vec{\sigma}) \right)^2 \right. \\ & \left. \left. + \left(\frac{F_{n\kappa}(r'(b', z'))}{r'(b', z')} \mathcal{Y}_{-\kappa m}(\Omega', \vec{\sigma}) \right)^2 \right] \right. \\ & \times \exp\left[-\frac{(b - b')^2}{2\beta_{pN}^2} \right] \int_0^{2\pi} d\phi_{b'} \\ & \left. \times \exp\left[\frac{-bb'}{\beta_{pN}^2} 2 \sin^2\left(\frac{\phi_b - \phi_{b'}}{2}\right) \right] \right\}. \quad (8) \end{aligned}$$

For numerical reasons, the z axis is chosen along the asymptotic direction of the ejectile. It is noteworthy that when computing the Dirac-Glauber phase $\mathcal{G}(\vec{b}, z)$ each of the residual nucleons behaves as a ‘‘frozen’’ scattering center with its unique relativistic wave function, which has an upper [$G(r)$] and lower [$F(r)$] component. Cylindrical symmetry about the axis defined by the ejectile’s asymptotic momentum makes the Dirac-Glauber phase to depend on the two independent variables (b, z) . Hereby, $b = |\vec{b}|$, where \vec{b} is orthogonal to the ejectile’s direction. Equation (8) includes the cumulative effect of free passage of the hit proton, single-scattering, double-scattering, up to and including $(A - 1)$ -fold scattering. Often,

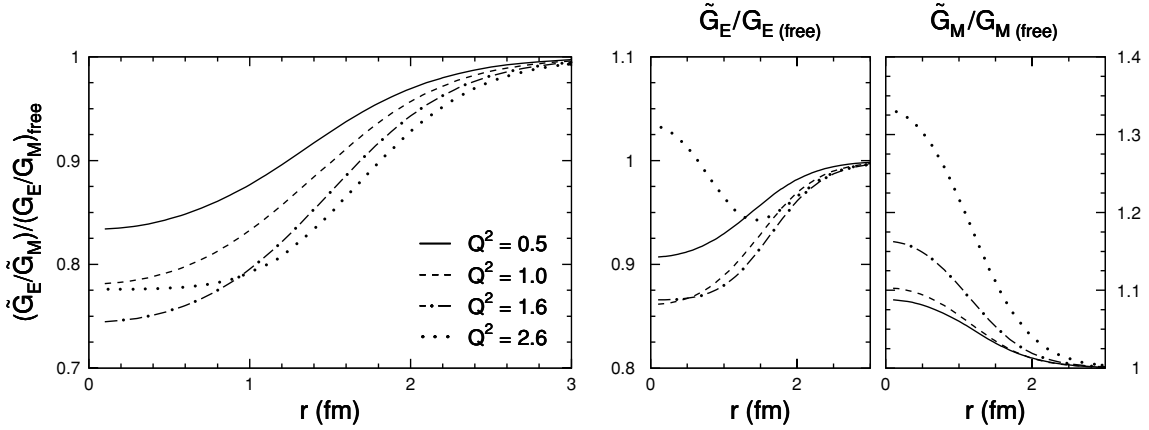


FIG. 1. QMC predictions [31] for the radial dependence of G_E , G_M , and G_E/G_M in ${}^4\text{He}$ at four different values of Q^2 (GeV/c) 2 . The bag radius was taken to be 0.8 fm.

the product over all scattering centers $\prod_{\alpha \neq \alpha_1}$ is approximated by a sum that is cut at some order in the multiple-scattering series. At the expense of a great numerical cost, we compute Eq. (8) rigorously.

B. Electromagnetic form factors

In the QMC model [29–31], the scalar (σ) and vector (ω) fields, carrying the forces between nucleons in quantum hadrodynamics [41,42], couple directly to the quarks within the nucleon. As a result, the intrinsic properties of a bound nucleon are affected by the presence of a medium. In the QMC framework, the nucleon is described in terms of the MIT bag model with almost massless and relativistic pointlike quarks. For the $A(\vec{e}, e'\vec{p})$ results presented below, we use the QMC predictions corresponding to a bag radius of 0.8 fm. In the QMC model, the electric and magnetic form factors attain a dependence on the total baryon density: $G_{E,M}(Q^2) \rightarrow G_{E,M}(\rho_B(\vec{r}), Q^2)$. In a mean-field model, the total baryon density $\rho_B(\vec{r})$ is defined according to the following:

$$\rho_B(\vec{r}) = \sum_{\alpha} \int d\vec{\sigma} (\phi_{\alpha}(\vec{r}, \vec{\sigma}))^{\dagger} (\phi_{\alpha}(\vec{r}, \vec{\sigma})). \quad (9)$$

The magnitude of the free form factors is not so well described within the QMC model. Therefore, we retain only the prediction for its density dependence and scale the free form factor with the ratio of the QMC form factors at a given density to the ones at vanishing baryon density as follows:

$$\tilde{G}_{E,M}^{\text{QMC}}(\rho_B(\vec{r}), Q^2) = G_{E,M}(Q^2) \frac{G_{E,M}^{\text{QMC}}(\rho_B(\vec{r}), Q^2)}{G_{E,M}^{\text{QMC}}(\rho_B(\vec{r})=0, Q^2)}. \quad (10)$$

In Fig. 1 the QMC predictions for the radial dependence of \tilde{G}_E , \tilde{G}_M , and their ratio in ${}^4\text{He}$ are displayed at four different values of Q^2 . Thereby, we have plotted the renormalized quantities as defined in Eq. (10). The magnitude of medium modifications grows with Q^2 . As suggested by Kelly in Ref. [18], the Q^2 dependence of the above ratios for a particular single-particle state can be estimated in the local density approximation in

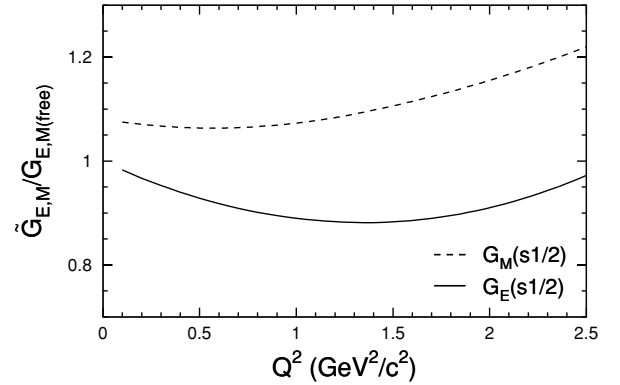


FIG. 2. The Q^2 dependence of the ratio of the in-medium to free electric and magnetic form factors for the proton in ${}^4\text{He}$ according to the QMC model with a bag radius of 0.8 fm [31].

terms of the following density convolution

$$\tilde{G}_{E,M}^{\text{QMC}}(\alpha_1, Q^2) = \frac{\int \tilde{G}_{E,M}^{\text{QMC}}(\rho_B(\vec{r}), Q^2) \rho_{\alpha_1}(\vec{r}) d\vec{r}}{\int \rho_{\alpha_1}(\vec{r}) d\vec{r}}. \quad (11)$$

Here, $\rho_{\alpha_1}(\vec{r})$ is the square of the $\langle A-1 | A \rangle$ overlap wave function. In a naive independent particle picture the overlap wave function corresponds with the single-particle wave function of the state from which the proton is ejected. Figure 2 displays $\tilde{G}_{E,M}^{\text{QMC}}(s1/2, Q^2)$ for a proton in ${}^4\text{He}$. At $Q^2 \geq 1.5$ (GeV/c) 2 , the averaged medium magnetic form factor is 10% larger than the free one. It has been pointed out that modifying the bag radius can considerably reduce the overall magnitude of the medium effects [46]. A recent calculation in the chiral quark soliton model resulted in predictions for the electromagnetic form factors of bound protons that show the same trends as the QMC model [47].

Recently, Yakhshiev *et al.* [39,40] addressed the issue of in-medium electromagnetic form factors in the framework of a modified Skyrme model. This model provides a fair description of nucleon properties in free space and adopts degrees of freedom directly related to the spontaneous chiral symmetry breaking of QCD. In contrast to most constituent quark models,

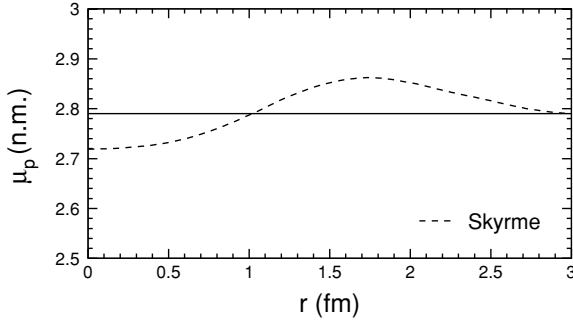


FIG. 3. The radial dependence of the proton magnetic moment in ${}^4\text{He}$ according to the Skyrme model of Ref. [40]. The free case corresponds with $\mu_p = 2.79$ n.m.

the pion-cloud contribution is naturally taken into account. As a result, the influence of the nuclear medium and the nucleon's response to it are predicted to be very probe dependent. Beyond $Q^2 = 0.6$ (GeV/c)², vector mesons and boost effects are deemed to come into play, and the Skyrme model is no longer considered realistic. In the Skyrme model, the proton magnetic moment gains an additional radial dependence dictated by the density of the nucleus. Whereas $G_E(Q^2)$ remains unaffected, its magnetic counterpart takes on the following form:

$$G_M(Q^2, r) = \mu_p(r)G_E(Q^2). \quad (12)$$

In Fig. 3 the medium proton magnetic moment is displayed as a function of the distance to the center of the ${}^4\text{He}$ nucleus. In the interior of ${}^4\text{He}$, the magnetic form factor is mildly suppressed, whereas a modest increment is observed in the surface area.

When including medium modifications in the $A(\vec{e}, e'\vec{p})$ calculations, the electromagnetic current operator of Eq. (4) is modified according to the following:

$$J^\mu(\vec{r}) = \tilde{F}_1^p(\rho_B(\vec{r}), Q^2)\gamma^\mu + \tilde{F}_2^p(\rho_B(\vec{r}), Q^2)i\frac{\kappa_p}{2m_p}\sigma^{\mu\nu}q_\nu. \quad (13)$$

The density-dependent Dirac and Pauli form factors are related to the $\tilde{G}_E^{\text{QMC}}(\rho_B(\vec{r}), Q^2)$ and $\tilde{G}_M^{\text{QMC}}(\rho_B(\vec{r}), Q^2)$ of Eq. (10) in the standard fashion. The medium-modified form factors $\tilde{F}_{1,2}^p$ in Eq. (13) depend on the total density in the neighborhood of the nucleon that absorbs the virtual photon.

III. RESULTS

All ${}^4\text{He}(\vec{e}, e'\vec{p})$ and ${}^{16}\text{O}(\vec{e}, e'\vec{p})$ calculations reported in this section are performed in quasielastic kinematics and adopt kinematical conditions that allow a direct comparison with the available data from Refs. [20–22]. For the ${}^4\text{He}$ nucleus, the polarization-transfer measurements have been performed in parallel kinematics.

Throughout this section, we adopt a dipole parametrization for the free-nucleon form factors. This choice may appear doubtful as improved fits implementing the new $p(\vec{e}, e'\vec{p})$ data are readily available [48]. For the present purposes, however, a dipole parametrization is adequate. Indeed, the ${}^{16}\text{O}(\vec{e}, e'\vec{p})$ data are restricted to $Q^2 = 0.8$ (GeV/c)², where deviations between the dipole and more sophisticated parametrizations

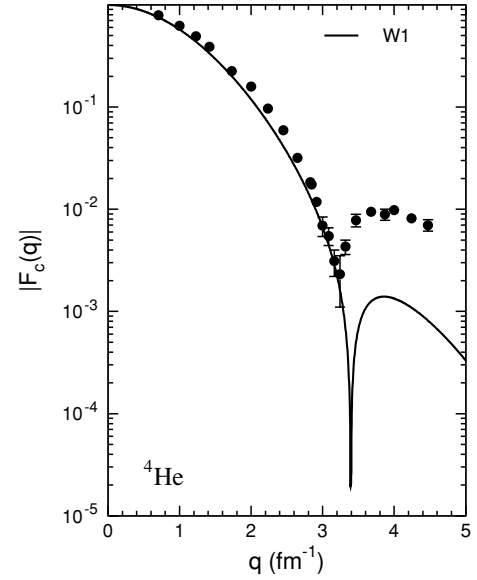


FIG. 4. The charge form factor of ${}^4\text{He}$, obtained within the W1 parametrization of [43]. The data are from Refs. [49] and [50].

are minor. Conversely, the ${}^4\text{He}$ polarization-transfer results are commonly expressed in terms of a double ratio R

$$R = \frac{(P'_x/P'_z)_{{}^4\text{He}}}{(P'_x/P'_z)_{{}^1\text{H}}}, \quad (14)$$

which is almost independent of the used parametrization for the form factors, as long as identical ones are used for ${}^4\text{He}$ and ${}^1\text{H}$. To not obscure the result by small kinematical differences between the individual ${}^1\text{H}$ and ${}^4\text{He}$ measurements, data and calculations are often shown in terms of a double ratio with the RPWIA result as baseline.

At present, realistic relativistic wave functions for the ${}^4\text{He}$ ground state are not available. Wave functions based on a relativistic mean-field approach emerge as the only alternative when embarking on fully relativistic $A(e, e'p)$ calculations. At first sight, an independent-particle approximation for describing the four-nucleon system may appear as a venture into dangerous territory. As can be appreciated from Fig. 4, however, a fair description of the low-momentum part of the charge form factor for the ${}^4\text{He}$ nucleus is obtained with the “W1” parametrization used throughout this work. The deviation between the computed and measured charge form factor F_c at high momentum transfer can be partly attributed to large two-body charge contributions [51], which are neglected for the curve displayed in Fig. 4.

A source of theoretical uncertainty on the computed polarization-transfer components is the presence of short-range correlations (SRC). The RMSGA formalism outlined in Sec. II A is based on an independent-particle approximation. The effect of SRC on the FSI mechanisms can be estimated by introducing a central correlation function in the expression for the Dirac-Glauber phase of Eq. (6). This amounts to performing the following substitution:

$$|\phi_\alpha(\vec{r}')|^2 \rightarrow |\phi_\alpha(\vec{r}')|^2 g(\vec{r} - \vec{r}'), \quad (15)$$

where $g(\vec{r} - \vec{r}')$ is the central correlation function. Physically, the existence of a central correlation function reflects the inability of mean-field models to properly implement the strong repulsion of the nucleon-nucleon force at short internucleon distances. We use the central correlation function from a G-matrix calculation by Gearheart and Dickhoff [52]. To date, the strongest sensitivity to central correlation functions is observed in exclusive $A(e, e'pp)$ reactions. The adopted correlation function provides a favorable agreement with the $^{12}\text{C}(e, e'pp)$ and $^{16}\text{O}(e, e'pp)$ data [53]. In the process of computing the Dirac-Glauber phase of Eq. (8), the introduction of a correlation function through the replacement of Eq. (15), strongly reduces the interaction between the struck proton and any of the scattering centers when they are very close (internucleon distances smaller than 0.8 fm) and bring about a moderate enhancement for internucleon distances between 0.8 and 2 fm. In Fig. 5, we investigate the effect of SRC on the transferred-polarization components in ^4He at two different values of Q^2 . The results are expressed in the barycentric frame with l parallel to the direction of the ejectile \vec{p}_f and t in the hadronic plane, orthogonal to the l component. As we can see, the SRC effects are relatively small, being typically of the order of 1% at a missing momentum of 200 MeV/c. Some asymmetric effect on P'_t and P'_l is seen. A major finding is that the effect of SRC on the Dirac-Glauber phase tends to cancel in the ratio R at smaller values of Q^2 . At higher values, we predict a modest enhancement of R due to SRC effects.

We now turn to the results for the double-polarization ratio R obtained for the ^4He nucleus. Response functions from the model calculations were used in a Monte Carlo code [54] to calculate the transferred and induced proton polarizations averaged over the experimental acceptance. The starting point is always the huge number of events (experimental data or MC simulations) within the acceptance of the detectors. The full acceptance is then divided in various bins. For Figs. 6 and 7 there are four bins in p_m for the data and several more for the calculations. Next, the average value of the polarization is calculated for each bin. For the p_m distributions the data are reported at the mean value of the missing momentum within that bin. The best comparison with the model would be to bin

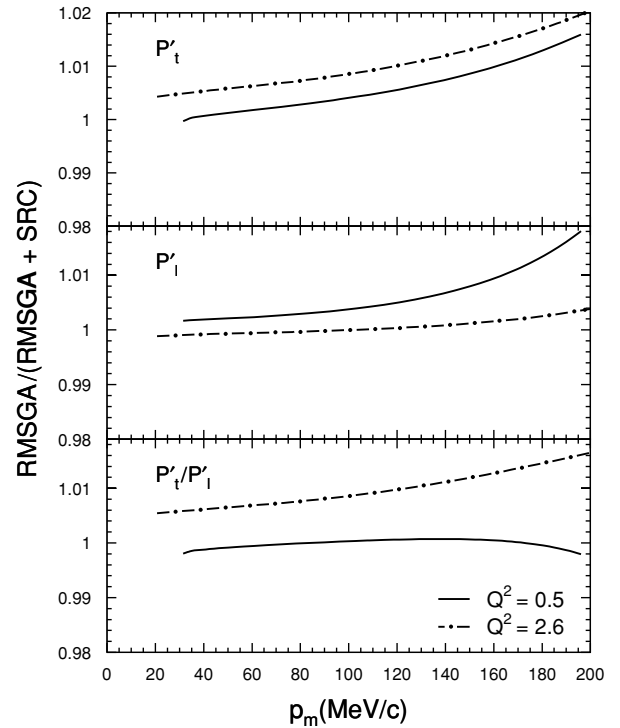


FIG. 5. Relative effect of short-range correlations on the polarization-transfer components and their ratio. The solid (dot-dashed) curves refer to $^4\text{He}(\vec{e}, e'\vec{p})$ in quasielastic and parallel kinematics for $Q^2 = 0.5(2.6)$ (GeV/c^2). The RMSGA + SRC results implement the effect of SRC according to the prescription of Eq. (15).

the MC data into the same number of bins as the data. One would then compare one data point with one calculated point. That way, however, the reader loses the information about the general missing momentum dependence. Our comparison is reliable as long as the transferred polarizations are not changing rapidly within the considered bin width.

Figure 6 shows R as a function of the missing momentum at $Q^2 = 0.4$ and 0.5 (GeV/c^2). We note that positive missing momentum p_m corresponds to $|\vec{p}_f| < |\vec{q}|$. As can be inferred,

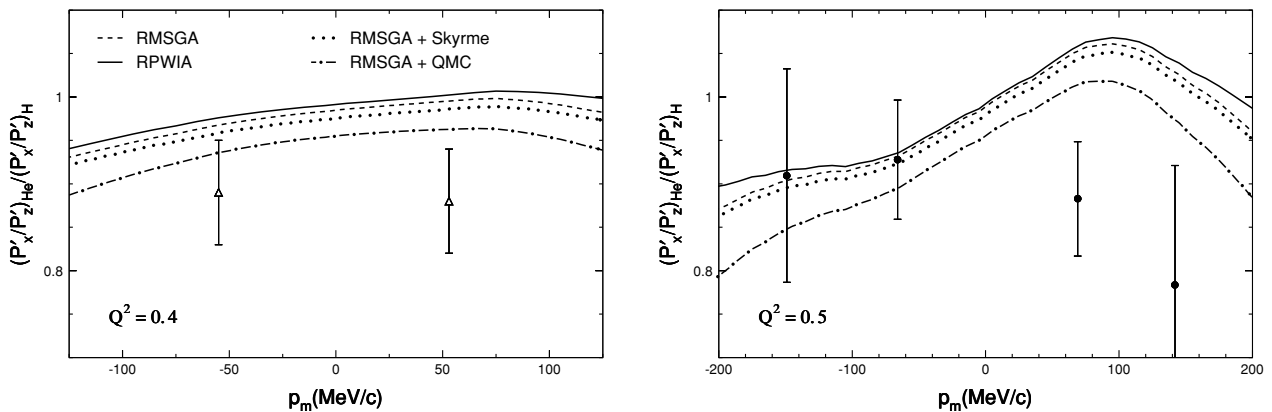


FIG. 6. The double ratio R as a function of the missing momentum for $Q^2 = 0.4$ and 0.5 (GeV/c^2) in ^4He . The solid (dashed) curve are RPWIA (RMSGGA) calculations. Influence of medium modifications are shown for the QMC (dot-dashed) and the Skyrme model (dotted). Data points are from [21](open triangles) and [22] (solid circles).

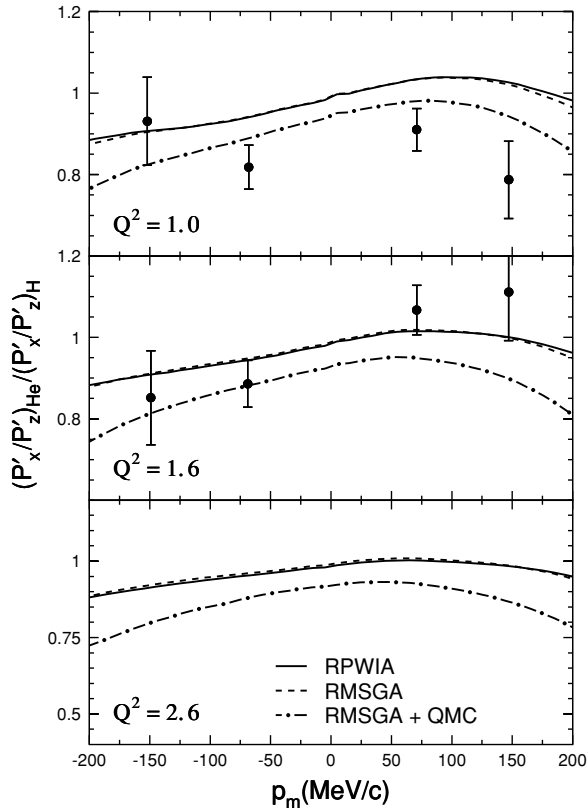


FIG. 7. The double ratio R as a function of the missing momentum at three values of Q^2 in ${}^4\text{He}$. The solid (dashed) curve are RPWIA (RMSGa) calculations, whereas the dot-dashed curve represents RMSGA calculations including in-medium electromagnetic form factors of the QMC model. Data points are from Ref. [22].

the FSI have only a minor impact on R , but move the predictions somewhat closer to the measurements. Both RMSGA and RPWIA overestimate the double ratio R by nearly 10% and predict $R \approx 1$ for zero recoil momentum. After implementing the medium-modified electromagnetic form factors from the QMC model, the computed double-ratios R are lowered by almost 8%, resulting in a better overall agreement with the data. The Skyrme model predicts modest medium modifications that do not suffice to bring about a major improvement in the description of the data within the context of the RMSGA model.

Figure 7 summarizes the missing momentum dependence of the ${}^4\text{He}$ results for $Q^2 \geq 1$ (GeV/c)² [22]. The FSI effects on R are even smaller in this high-energy regime. For $Q^2 = 1.6$ (GeV/c)² the measured p_m dependence can be reasonably reproduced using free-nucleon form factors. Substituting the free form factors with the QMC ones reduces R , an effect that grows with p_m . At $Q^2 = 1.0$ (GeV/c)² the effect of medium modifications moves the theoretical curves closer to the data. Qualitatively our RMSGA results are not dramatically different from the RDWIA predictions presented in [22].

In Fig. 8, the superratio R/R_{RPWIA} is displayed as a function of Q^2 . Also here, the data and calculations are integrated over the full experimental acceptance. The data and calculations

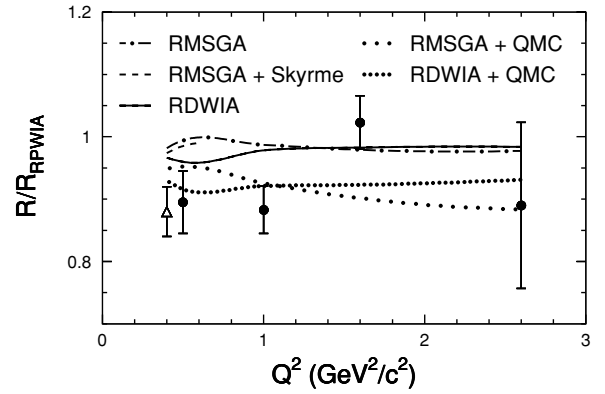


FIG. 8. The superratio R/R_{RPWIA} as a function of Q^2 in ${}^4\text{He}$. The dot-dashed (solid) curve shows RMSGA (RDWIA) calculations, and the dotted (dashed) curve represents RMSGA calculations with in-medium electromagnetic form factors from the QMC (Skyrme) model. The RDWIA and RDWIA+QMC results are those from the Madrid group as reported in Ref. [22]. Data are from Refs. [21] (open triangle) and [22] (solid circles).

are reported as single points at the nominal Q^2 value. The model “curves” only connect the computed points to guide the eye. As seen in Fig. 8 the Mainz data point nicely matches with the lowest Q^2 measurement at JLAB. As off-shell effects are not completely negligible for the polarization-transfer components, it is worth stressing that the RDWIA (RMSGa) ${}^4\text{He}$ results shown here are obtained with the $CC1$ ($CC2$) current operator. For $Q^2 \leq 1$ (GeV/c)² the standard nuclear physics RDWIA and RMSGA results fail to reproduce the ratio R . The overestimation is of the order of 10% for RMSGA, and 5–7% in RDWIA. The predicted four-momentum dependence for R is modest in both models. The RMSGA attributes smaller effects to FSI than RDWIA does. In Ref. [38], a similar trend was found when comparing RDWIA and RMSGA $A(e, e'p)$ nuclear transparencies for light nuclei.

Inclusion of medium modifications for the electromagnetic form factors according to the predictions of the Skyrme model shifts the RMSGA calculations marginally closer to the data. The results for the Skyrme model are shown up to $Q^2 = 0.6$ (GeV/c)² because the model is no longer deemed realistic at higher values. Conversely, implementing QMC electromagnetic form factors lowers the p_m -integrated RMSGA predictions for the superratio R between 5 and 10%. The difference between the RMSGA and the RMSGA+QMC values for P'_x/P'_z grows with increasing Q^2 . This reflects the fact that in the QMC model, the ratio \tilde{G}_E/\tilde{G}_M moves steadily away from the free values with increasing Q^2 to reach a maximum of over 20% at about $Q^2 = 2$ (GeV/c)², after which some turning in the trend is observed. This has been illustrated in Fig. 9. As can be inferred from this picture, about one-third of the predicted magnitude of the medium modifications on G_E/G_M is visible in the P'_x/P'_z ratio. It is worth stressing that Fig. 9 compares two different quantities. On the one hand, the curve showing the \tilde{G}_E/\tilde{G}_M has been averaged over the squared $1s1/2$ proton overlap wave function, thus receiving its largest contributions from the nuclear interior. This is not

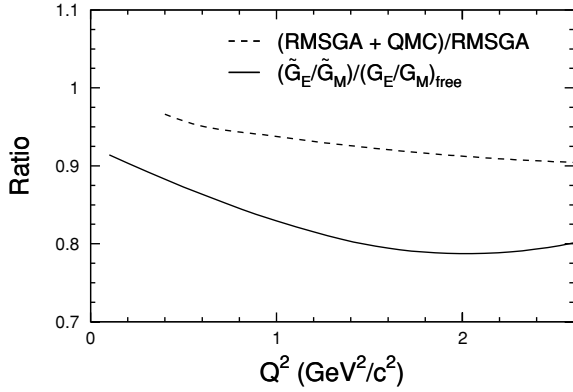


FIG. 9. The ratio of the RMSGA+QMC to the RMSGA prediction for R as a function of Q^2 for the $1s_{1/2}$ proton in ^4He (dashed line). The solid line shows $[\tilde{G}_E^{\text{QMC}}(1s_{1/2}, Q^2)/\tilde{G}_M^{\text{QMC}}(1s_{1/2}, Q^2)]/[G_E(Q^2)/G_M(Q^2)]$.

necessarily the case for the $^4\text{He}(\bar{e}, e' \bar{p})$ observables. Indeed, in the process of computing the observables, the medium effects in the form factors are weighted with a more complex function that involves not only the $1s_{1/2}$ proton overlap wave function but also the current operator and the scattering wave function. The dashed curve of Fig. 9 indicates that over the whole larger radii, and correspondingly lower densities, are probed. This phenomenon reduces the magnitude of the medium-dependent effects on the observables.

Figure 10 displays the induced normal polarization as a function of Q^2 for the ^4He nucleus. In the one-photon exchange approximation, P_y vanishes in the absence of FSI. Accordingly, this observable serves as a stringent test for

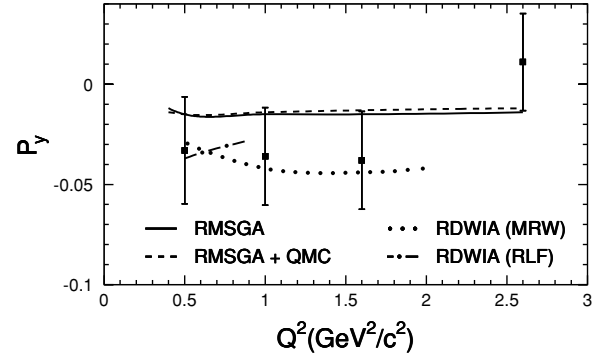


FIG. 10. The induced normal polarization as a function of Q^2 in ^4He . The solid curve represents RMSGA calculations with free form factors. For the dashed lines $\tilde{G}_{E,M}^{\text{QMC}}(1s_{1/2}, Q^2)$ form factors are used. Data points and RDWIA results are from Ref. [22].

models of FSI mechanisms. The smallness of P_y suggests relatively moderate FSI. The RDWIA calculations for P_y are shown for exactly the same kinematics, although with the $CC1$ choice for the current operator. The RDWIA predictions for the P_y in $^4\text{He}(e, e' \bar{p})$ are presented for two viable choices of the optical-potential parametrization: “RLF” (limited to proton lab kinetic energies smaller than 0.4 GeV) and “MRW” (limited to proton lab kinetic energies smaller than 1.0 GeV). The two optical potentials predict a dissimilar Q^2 dependence for P_y . Indeed, in many cases various optical potentials can fit the elastic proton-nucleus data equally well, but do not necessarily lead to identical predictions in electromagnetically induced nucleon knockout. The RDWIA model predicts values for P_y

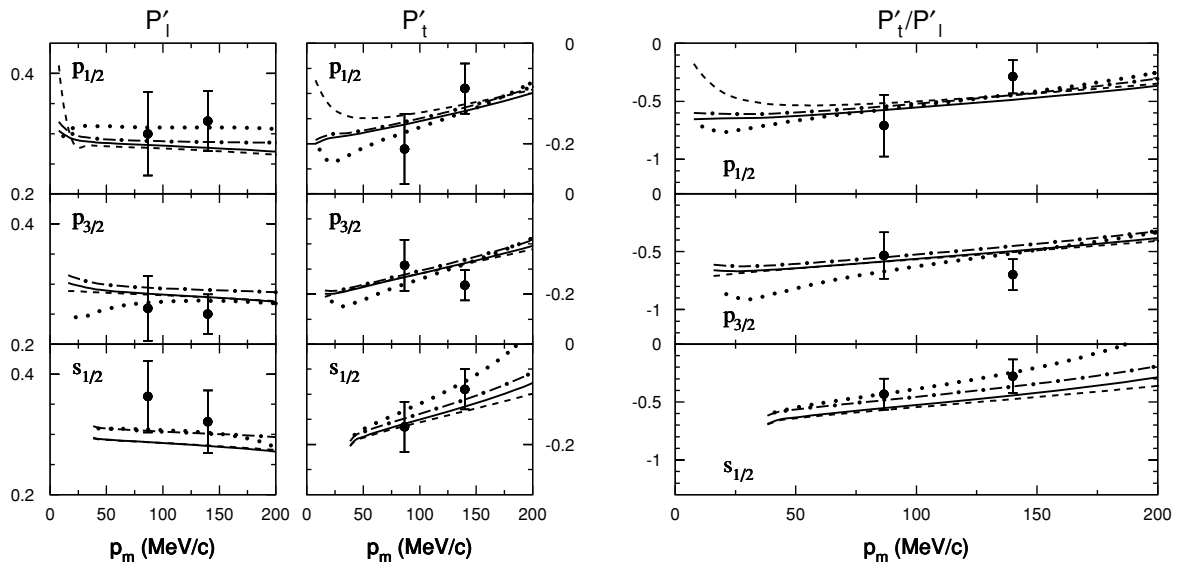


FIG. 11. Transferred polarization components for proton knockout from the three shells in ^{16}O for $Q^2 = 0.8 (\text{GeV}/c)^2$ in constant (\vec{q}, ω) kinematics. The solid (dashed) curve represents RMSGA (RPWIA) calculations with free-nucleon form factors, whereas the dot-dashed curve is obtained from RMSGA calculations when using the QMC form factors. The dotted curve represents RDWIA calculations. Data points are from [20].

that are over twice as large as the RMSGA ones. Studies in the Dirac eikonal approach have stressed the importance of the spin-orbit part in the optical potential for the computed values of P_y in ${}^{16}\text{O}$ [56]. Similar observations have been made for the ${}^{12}\text{C}(e, e'\vec{p})$ case at $Q^2 = 0.49$ (GeV/c) 2 [57]. The measured value of P_y at $Q^2 = 2.6$ (GeV/c) 2 may indeed suggest the decreasing role of this spin-dependent part as the energy increases. As can be inferred, P_y remains nearly unaffected by medium modifications in the electromagnetic form factors. This is not unexpected given that P_y is an observable which quantifies the magnitude of secondary processes, like rescattering mechanisms. The introduction of medium-modified form factors induces some change in the way these mechanisms are folded over the density of the target nucleus.

Finally, in Fig. 11, results for the transferred polarization components and their ratio for the ${}^{16}\text{O}$ nucleus are shown at $Q^2 = 0.8$ (GeV/c) 2 . Hereby, we adopt constant (\vec{q}, ω) kinematics and compare the RMSGA predictions with the measurements of Ref. [20] and the results of the RDWIA model from the Madrid group. For the oxygen calculations, the RDWIA and RMSGA calculations adopt identical mean-field wave functions (W1 parametrization) and current operators (CC2 in the Coulomb gauge). The RDWIA calculations are performed with the EDAD1 parametrization for the optical potential [58]. In essence, the RDWIA and RMSGA curves result from identical model ingredients, apart from the implementation of FSI distortions, which is grounded on different philosophies. The RPWIA and RMSGA curves for P'_i and P''_i are close, the RDWIA model predicting larger FSI distortions. At corresponding Q^2 values (Figs. 6 and 7), the ${}^4\text{He}$ results could be better reproduced after introducing QMC medium-modified form factors. As can be appreciated from Fig. 11, the ${}^{16}\text{O}$ data do not allow one to draw conclusions on the possibility of medium modifications. The overall trends of the ${}^{16}\text{O}$ polarization-transfer data are reasonably reproduced in the RMSGA, using free-proton electromagnetic form factors. When comparing the RMSGA and RMSGA+QMC curves, a significant orbital dependence of the magnitude of the medium effect is observed. Comparing the results for R for the various orbitals in a particular nucleus could allow one to study the density dependence of the medium effects.

IV. CONCLUSIONS

Unfactorized and relativistic Glauber calculations are performed for the polarization-transfer components in ${}^4\text{He}$ and ${}^{16}\text{O}(\vec{e}, e'\vec{p})$ for $Q^2 = 0.4, 0.5, 0.8, 1.0, 1.6,$ and 2.6 (GeV/c) 2 . The selected kinematics are those for which data are available. The adopted framework has the virtues that it is relativistic and can be reliably applied up to the highest four-momentum transfers covered in the measurements. Overall, the effect of FSI on the polarization-transfer components is smaller in the relativistic Glauber framework than in a relativistic optical-potential framework. After all, this is not so surprising given that typical Glauber approaches rely on spin-independent nucleon-nucleon scattering amplitudes when modeling the final-state interactions. The spin-dependent effects are expected to lose their importance as the energy increases. Polarization studies with the electromagnetic probe, such as the one presented here, will help in further clarifying this issue.

For the ${}^{16}\text{O}$ target, for which the data are restricted to $Q^2 = 0.8$ (GeV/c) 2 , the calculations provide a fair description when adopting free-proton electromagnetic form factors. A similar situation holds for the ${}^4\text{He}$ case at $Q^2 \geq 1.6$ (GeV/c) 2 . For ${}^4\text{He}$ and $Q^2 \leq 1.0$ (GeV/c) 2 substantial deviations between the RMSGA predictions and the data are observed. Under these circumstances, the implementation of the in-medium form factors from the QMC nucleon model, makes the RMSGA calculations to go in the right direction and induces changes in the ratio of the polarization-transfer components, which are of the right order of magnitude to explain the discrepancies. A recently approved experiment at JLAB [55] will address the polarization-transfer ratio at Q^2 values of 0.8 and 1.3 (GeV/c) 2 and is expected to reduce the statistical uncertainties by over a factor of two compared to the previous round of measurements.

ACKNOWLEDGMENTS

We thank J. M. Udías and M. C. Martínez for providing us with the RDWIA calculations and for numerous discussions. This work is supported by the Fund for Scientific Research (FWO), the research council of Ghent University, and by the U.S. Department of Energy under Grant DE-FG02-95ER40901.

-
- [1] J. R. Smith and G. A. Miller, Phys. Rev. Lett. **91**, 212301 (2003).
 - [2] J. Carlson, J. Jourdan, R. Schiavilla, and I. Sick, Phys. Lett. **B553**, 191 (2003).
 - [3] J. Morgenstern, and Z.-E. Meziani, Eur. Phys. J. A **17**, 451 (2003).
 - [4] I. Sick, Phys. Lett. **B157**, 13 (1985).
 - [5] E. M. Henley and G. Krein, Phys. Lett. **B231**, 213 (1989).
 - [6] G. van der Steenhoven *et al.*, Phys. Rev. Lett. **57**, 182 (1986).
 - [7] D. Reffay-Pikeroen *et al.*, Phys. Rev. Lett. **60**, 776 (1988).
 - [8] J. Ryckebusch, K. Heyde, D. Van Neck, and M. Waroquier, Phys. Lett. **B222**, 183 (1989).
 - [9] M. Buballa, S. Drodz, S. Krewald, and A. Szczurek, Phys. Rev. C **44**, 810 (1991).
 - [10] T. Warmann, and K. Langanke, Phys. Lett. **B273**, 193 (1991).
 - [11] J. E. Ducret *et al.*, Nucl. Phys. **A556**, 373 (1993).
 - [12] R. G. Arnold, C. E. Carlson, and F. Gross, Phys. Rev. **23**, 363 (1981).
 - [13] J.-M. Laget, Nucl. Phys. **A579**, 333 (1994).
 - [14] J. A. Caballero, T. W. Donnelly, E. Moya de Guerra, and J. M. Udias, Nucl. Phys. **A632**, 323 (1998).
 - [15] J. M. Udias, J. A. Caballero, E. Moya de Guerra, J. E. Amaro, and T. W. Donnelly, Phys. Rev. Lett. **83**, 5451 (1999).
 - [16] J. M. Udias and J. R. Vignote, Phys. Rev. C **62**, 034302 (2000).
 - [17] J. J. Kelly, Phys. Rev. C **59**, 3256 (1999).
 - [18] J. J. Kelly, Phys. Rev. C **60**, 044609 (1999).

- [19] H. W. L. Naus, S. J. Pollock, J. H. Koch, and U. Oelfke, Nucl. Phys. **A509**, 717 (1990).
- [20] S. Malov *et al.*, Phys. Rev. C **62**, 057302 (2000).
- [21] S. Dieterich *et al.*, Phys. Lett. **B500**, 47 (2001).
- [22] S. Strauch *et al.*, Phys. Rev. Lett. **91**, 052301 (2003).
- [23] J. Ryckebusch, D. Debruyne, W. Van Nespen, and S. Janssen, Phys. Rev. C **60**, 034604 (1999).
- [24] A. Meucci, C. Giusti, and F. D. Pacati, Phys. Rev. C **64**, 014604 (2001).
- [25] M. Radici, A. Meucci, and W. H. Dickhoff, Eur. Phys. J. A **17**, 65 (2003).
- [26] F. K. Tabatabaei, J. E. Amaro, and J. A. Caballero, Phys. Rev. C **68**, 034611 (2003).
- [27] M. C. Martinez, J. R. Vignote, J. A. Caballero, T. W. Donnelly, E. Moya de Guerra, and J. M. Udias, Phys. Rev. C **69**, 034604 (2004).
- [28] J. M. Udias, P. Sarriguren, E. Moya de Guerra, E. Garrido, and J. A. Caballero, Phys. Rev. C **48**, 2731 (1993).
- [29] P. A. M. Guichon, Phys. Lett. **B200**, 235 (1988).
- [30] D. H. Lu, A. W. Thomas, K. Tsushima, A. G. Williams, and K. Saito, Phys. Lett. **B417**, 217 (1998).
- [31] D. H. Lu, K. Tsushima, A. W. Thomas, A. G. Williams, and K. Saito, Phys. Rev. C **60**, 068201 (1999).
- [32] R. Glauber and G. Matthiae, Nucl. Phys. **B21**, 135 (1970).
- [33] S. J. Wallace, Phys. Rev. C **12**, 179 (1975).
- [34] D. Yennie, in *Hadronic Interactions of Electrons and Photons*, edited by J. Cummings and D. Osborn (Academic, New York, 1971), p. 321.
- [35] D. Debruyne and J. Ryckebusch, Nucl. Phys. **A699**, 65 (2002).
- [36] D. Debruyne, J. Ryckebusch, S. Janssen, and T. Van Cauteren, Phys. Lett. **B527**, 62 (2002).
- [37] J. Ryckebusch, D. Debruyne, P. Lava, S. Janssen, B. Van Overmeire, and T. Van Cauteren, Nucl. Phys. **A728**, 226 (2003).
- [38] P. Lava, M. C. Martinez, J. Ryckebusch, J. A. Caballero, and J.M. Udias, Phys. Lett. **B595**, 177 (2004).
- [39] U. T. Yakhshiev, M. M. Musakhanov, A. M. Rakhimov, U.-G. Meißner, and A. Wirzba, Nucl. Phys. **A700**, 403 (2002).
- [40] U. T. Yakhshiev, U.-G. Meißner, and A. Wirzba, Eur. Phys. J. A **16**, 569 (2003).
- [41] B. Serot, and J. Walecka, Adv. Nucl. Phys. **16**, 1 (1986).
- [42] J. D. Walecka, Ann. Phys. **83**, 491 (1974).
- [43] R. Furnstahl *et al.*, Nucl. Phys. **A615**, 441 (1997).
- [44] T. de Forest, Nucl. Phys. **A392**, 232 (1983).
- [45] K. Hagiwara *et al.*, Phys. Rev. D **66**, 010001 (2002), <http://pdg.lbl.gov/>.
- [46] D. H. Lu, A. W. Thomas, and A. G. Williams, Phys. Rev. C **57**, 2628 (1998).
- [47] Jason R. Smith and Gerald A. Miller, Phys. Rev. C (to be published), nucl-th/0407093.
- [48] H. Budd, A. Bodek, and J. Arrington, hep-ex/0308005 and J. Arrington, Phys. Rev. C **69**, 022201(R) (2004).
- [49] R. Frosch, J. McCarthy, R. Rand, and M. Yearian, Phys. Rev. **160**, 874 (1967).
- [50] J. C. McCarthy, I. Sick, and R. R. Whitney, Phys. Rev. C **15**, 1396 (1977).
- [51] J. Carlson and R. Schiavilla, Rev. Mod. Phys. **70**, 743 (1998).
- [52] C. Gearheart, Ph.D. thesis, Washington University, St. Louis, 1994.
- [53] J. Ryckebusch, and W. Van Nespen, Eur. Phys. J. A **20**, 435 (2004).
- [54] P. Ulmer, MCEEP, Monte Carlo for Electro-Nuclear Coincidence Experiments, Program Version 3.4 (2000).
- [55] Jefferson Lab Experiment E03-104, Probing the Limits of the Standard Model of Nuclear Physics with ${}^4\text{He}(\vec{e}, e'\vec{p}){}^3\text{H}$ Reaction, R. Ent, R. Ransome, S. Strauch, and P.E. Ulmer, spokespeople.
- [56] Hiroshi Ito, S. E. Koonin, and Ryoichi Seki, Phys. Rev. C. **56**, 3231 (1997).
- [57] R. J. Woo *et al.*, Phys. Rev. Lett. **80**, 456 (1998).
- [58] M. C. Martinez (private communication).